

This discussion paper is/has been under review for the journal Atmospheric Chemistry and Physics (ACP). Please refer to the corresponding final paper in ACP if available.

Insights into the chemical composition of summertime PM_{2.5} at the northeast of the Qinghai-Xizang (Tibet) Plateau

J. Xu¹, Q. Zhang², Z. Wang¹, G. Yu¹, X. Ge², and X. Qin¹

¹Qilian Shan Station of Glaciology and Ecologic Environment, State Key Laboratory of Cryospheric Sciences, Cold and Arid Regions Environmental and Engineering Research Institute, CAS, Lanzhou 730000, China

²Department of Environmental Toxicology, University of California, Davis, California 95616, USA

Received: 30 November 2014 – Accepted: 23 December 2014 – Published: 15 January 2015

Correspondence to: J. Xu (jzxu@lzb.ac.cn)

Published by Copernicus Publications on behalf of the European Geosciences Union.

ACPD

15, 1307–1341, 2015

Insights into the
chemical
composition of
summertime PM_{2.5}

J. Xu et al.

Title Page

Abstract

Introduction

Conclusions

References

Tables

Figures

◀

▶

◀

▶

Back

Close

Full Screen / Esc

Printer-friendly Version

Interactive Discussion



Abstract

Aerosol filter samples were collected at a high-elevation mountain observatory in the northeastern part of the Qinghai-Xizang (Tibet) Plateau (QXP) during summer 2012 using a low-volume sampler and a micro-orifice uniform deposit impactor (MOUDI). The aim was to improve our understanding of the chemical composition of free tropospheric aerosols in the QXP region. The samples were analyzed for water-soluble inorganic ions (WSIs), organic carbon (OC), elemental carbon (EC), water soluble organic carbon (WSOC), and total organic nitrogen (TON). The bulk chemical composition and the average oxidation degree of water-soluble organic matter (WSOM) were assessed using a high resolution time-of-flight aerosol mass spectrometer. Furthermore, the concentrations of both primary organic aerosol (POA) and secondary organic aerosol (SOA) were estimated. The average mass concentration of the sum of the analyzed species in $\text{PM}_{2.5}$ (WSIs + OC + EC + TON) was $3.74 \mu\text{g m}^{-3}$, 36.2 % of which was sulfate, 17.8 % OC, 16.9 % nitrate, 10.1 % ammonium, 6.6 % calcium, 6.4 % TON, 2.6 % EC, 1.5 % sodium, 0.9 % chloride, 0.5 % magnesium, and 0.3 % potassium. The size distribution of sulfate and ammonium peaked in the accumulation mode ($0.32\text{--}0.56 \mu\text{m}$), whereas the size distributions of both nitrate and calcium peaked in the range of $1.8\text{--}3.2 \mu\text{m}$, suggesting the formation of nitrate on mineral dust. OC, EC and TON were also predominantly found in the accumulation mode. High average ratios of OC / EC (7.6) and WSOC / OC (0.79) suggested that organic aerosols were primarily made of secondary species. WSOM was found to be highly oxidized in all $\text{PM}_{2.5}$ samples with the average oxygen-to-carbon atomic ratio (O / C) being 1.16 and organic mass to carbon ratio (OM / OC) being 2.75. The highly oxidized WSOM was likely related to active cloud processing during upslope air mass transport coupled with strongly oxidizing environments caused by snow/ice photochemistry. SOA was estimated on average accounting for 75.3 % (46.4–96.4 %) of the $\text{PM}_{2.5}$, indicating that SOA accounted for a significant portion of the free tropospheric aerosols over the northern QXP.

Title Page

Abstract

Introduction

Conclusions

References

Tables

Figures

◀

▶

◀
Back

▶
Close

Full Screen / Esc

Printer-friendly Version

Interactive Discussion



1 Introduction

The Qinghai-Xizang (Tibet) Plateau (QXP), often called “the Third Pole” (Yao et al., 2012), is one of the most remote and isolated regions in the world. The high altitude of this region has long been recognized as ideal for studying the long-range transported

5 air pollutants. However, measurements from this area have been rare, usually due to the harsh natural condition and logistic difficulties. These restrictions have become less problematic in the last decade because of the development of mountain observatories and improvements in sampling instrumentation (Li et al., 2000; Cong et al., 2007; Bonasoni et al., 2008; Hegde and Kawamura, 2012; Sang et al., 2013).

10 Previous studies in the QXP region have focused on the chemical properties of aerosols and its source signature due to its important roles of aerosols in climate change. A few studies conducted at Himalayas revealed aerosols in this region is a complex mixture of inorganic and organic compounds (Carrico et al., 2003; Rengarajan et al., 2007; Decesari et al., 2010; Ram et al., 2010). Mineral dust was generally found to be an important constituent of aerosols in the QXP region because of the presence of large arid and semi-arid areas in “High Asia”. A relatively large proportion of carbonaceous aerosols was also observed when the region was influenced by air masses transported from South Asia, where widespread usage of biofuels has led to large emissions of biomass burning aerosols (Engling et al., 2011; Zhao et al., 2013). Indeed, analysis of the chemical compositions of snow pit samples collected 15 from a glacier in the central Himalayas indicated that biomass burning particles were significantly enhanced in snow during the winter – spring periods, due to transport of polluted air masses from northwest India and Nepal (Xu et al., 2013b).

20 Although the contributions of inorganic species (such as mineral dust) to aerosols in the QXP are important, their chemical process in the atmosphere are reasonably well characterized due to the small number of species involved and their relatively simple chemistry. There have been increased interests in the organic constituents of aerosol particles in recent years because of their high abundances, their complex chemical pro-

Title Page

Abstract

Introduction

Conclusions

References

Tables

Figures

◀

▶

◀
Back▶
Close

Full Screen / Esc

Printer-friendly Version

Interactive Discussion



cessing, and the importance in affecting the cloud properties (e.g., Kanakidou et al., 2005; Jimenez et al., 2009). Organic aerosol (OA) is usually dominated by secondary species in the remote region (Zhang et al., 2007) because of atmospheric aging processes during long-range transport. The oxidation degree of organic aerosol in the remote site, represented by the oxygen-to-carbon (O/C) atomic ratio, can be > 0.5 (e.g., Sun et al., 2009), which is similar to the O/C ratios that were found for oxygenated organic aerosol (OOA) in urban area decomposed by positive matrix factorization (PMF) analysis (Ulbrich et al., 2009; Zhang et al., 2011). However, the extent and the nature of the OA oxidation and secondary species are closely related to the source profiles and the aging processes it involved, and have never been carefully evaluated and determined in the QXP.

Most previous studies of aerosol chemistry at the QXP have been conducted in the Himalayan regions because of the key roles of Himalayas on regional climate and environment. There have been very few studies on aerosols reported from the northern QXP aerosols (Meng et al., 2013), despite their atmospheric behaviors might be significantly different from those found in the Himalayan regions because of the different climate pattern and aerosol sources in these two regions. For example, aerosols in the northern QXP mainly originate from the inland of China, whereas aerosols in the Himalayas mainly originate in India. Also, fine particles in the northern QXP contain large proportions of sulfate (Xu et al., 2014a; Zhang, N. et al., 2014), while fine particles in the Himalayas contain large proportions of carbonaceous material.

The Qilian Shan Station of Glaciology and Ecologic Environment (QSS) is situated on the northern slope of the western Qilian Shan Mountains, in the northeastern part of the QXP (Fig. S1). Due to the high elevation (4180 m a.s.l.) and long distance (200 km) from local pollution sources, the QSS is well suited for sampling background air masses. In addition, the QSS locates near the termini of several glaciers, making this area a unique local atmospheric environment within which the photochemistry of snow and glaciers has a relatively strong effect.

Insights into the chemical composition of summertime PM_{2.5}

J. Xu et al.

[Title Page](#)

[Abstract](#)

[Introduction](#)

[Conclusions](#)

[References](#)

[Tables](#)

[Figures](#)

◀

▶

[Back](#)

[Close](#)

[Full Screen / Esc](#)

[Printer-friendly Version](#)

[Interactive Discussion](#)



In our previous studies, the seasonal variations of mass concentration of water soluble ions and the number concentration of particles have been characterized (Xu et al., 2013a, 2014a), which presented two maxima in spring and summer, respectively. The first maximum corresponded to the period during which dust storms predominantly occur in North China, while the second peak corresponded to the period when the thermal circulation between areas of high and low elevation is strongest, which the prevailing valley wind in the northeast of the QSS blew the polluted air masses to this region. In the present study, we performed an intensive field measurement study during the summer of 2012 with the aim of determining the chemical characteristics and sources of fine aerosols at QSS during summer period. Here, we investigated the PM_{2.5} chemical compositions and the properties of the associated organic chemical species, such as elemental ratios, by applying a suite of instruments including a high resolution time-of-flight mass spectrometer (HR-ToF-AMS). The elemental ratios of organic species are very valuable in understanding the oxidation state of OA and thus the aging processes that had occurred during its long-range transport. The size distributions of the chemical species were also assessed to provide insights into the sources and chemical processes of aerosol.

2 Sample collection and analysis

2.1 Aerosol sampling

The samples were collected at the QSS atmospheric chemistry observatory (39.50° N, 96.51° E; 4180 m a.s.l., Fig. S1). The sampling site and the QSS were described in detail by Xu et al. (2013). The summer climate at the QSS is dominated by the East Asian monsoon, which brings about half of the annual precipitation. This study was conducted from 11 July to 6 September 2012. PM_{2.5} samples were collected using a low-volume (16.7 L min⁻¹ flow rate) aerosol sampler (BGI, USA, model PQ 200), powered by solar cells. The instrument was regularly calibrated using a TetraCal® calibrator (BGI, USA).

Insights into the chemical composition of summertime PM_{2.5}

J. Xu et al.

Title Page

Abstract

Introduction

Conclusions

References

Tables

Figures

◀

▶

◀

▶

Back

Close

Full Screen / Esc

Printer-friendly Version

Interactive Discussion



All samples were collected on 47 mm quartz fiber filters (Whatman, Maidstone, England). The flow rate was measured at 5 min intervals by an internal volume flow meter, and the recorded flow data were used to calculate the volume of air sampled. Meteorological parameters including wind speed, wind direction, temperature, precipitation, and relative humidity were recorded at 30 min intervals at the meteorological station at the QSS, and the recorded data were used to calculate the air volume sampled at standard conditions (1013 hPa, 273 K). Collection of each sample was started in the morning and continued for 3 d, and a total of 19 aerosol filter samples were obtained. Three procedure blanks were collected in the field to allow any contamination that occurred during sampling preparation, transportation, and storage to be quantified. The sampling volume at the standard conditions ranged from 42 to 44 m³, with a mean ($\pm 1\sigma$) value of 43.2 ± 0.5 m³. It should be noted that the mass concentrations reported here are based on volume at the standard conditions.

In addition, measurements to determine the size distribution of chemical species were made at the QSS from 21 July to 4 September 2012. A 10-stage multi-nozzle micro orifice uniform deposit impactor (MOUDI, Model R110, MSP Corp., Shoreview, MN) was used to sample particles at a flow rate of 30 L min⁻¹ over a size range of 0.056–18 µm with nominal cut offsets of 0.056, 0.10, 0.18, 0.32, 0.56, 1.0, 1.8, 2.5, 5.6, 10, and 18 µm. The air pump was calibrated before each sample was collected and the pump was closely monitored to identify any changes of the flow rate. The collection substrates were 47 mm quartz fiber filters which had been heated at 500 °C for 8 h prior to sample collection so as to remove all possible organic material. The sampling time varied between ~20 and ~120 h depending on the weather conditions. A total of four sets of filters were obtained. All the filters were placed in individual aluminum-lined plastic boxes and stored at –15 °C prior to analysis.

2.2 Chemical analysis

The samples were analyzed to characterize their chemical compositions using a series of instruments, namely ion chromatography (IC) instruments, a total water soluble

J. Xu et al.

Title Page

Abstract

Introduction

Conclusions

References

Tables

Figures

◀

▶

Back

Close

Full Screen / Esc

Printer-friendly Version

Interactive Discussion



organic carbon/total nitrogen (TOC/TN) analyzer, a HR-ToF-AMS, and an organic carbon/element carbon (OC/EC) analyzer. For each OC/EC analysis, a piece of filter measuring 0.526 cm^2 was punched from a sample filter and analyzed directly using the instrument. The rest of that filter was extracted by sonication in 15 mL deionized water for 30 min at $\sim 0^\circ\text{C}$, and the extract was immediately filtered using a $0.45\text{ }\mu\text{m}$ Acrodisc syringe filters (Pall Life Sciences, Ann Arbor, MI, USA).

2.2.1 IC analysis

Eight ionic species (Na^+ , NH_4^+ , K^+ , Ca^{2+} , Mg^{2+} , Cl^- , NO_3^- , and SO_4^{2-}) were determined using two IC system (881 Compact IC Pro, Metrohm, Herisau, Switzerland). One of the IC systems was used to determine cations, and was equipped with a Metrosep C4 guard/2.0 column and Metrosep C4 250/2.0 column (Metrohm), which were kept at 30°C during measurements. The other IC system, equipped with a Metrosep RP2 guard/3.6 column and a Metrosep A Supp15 250/4.0 column (Metrohm), and kept at 45°C during measurements, was used to determine anions. The mobile phase in the cation IC system was 1.75 mM nitric acid (made from 70 % nitric acid, Sigma-Aldrich, St Louis, MO, USA) and 0.75 mM dipicolinic acid (made from $\geq 99.5\%$ pure dipicolinic acid, Sigma-Aldrich), and eluted at a flow rate of 0.3 mL min^{-1} . The eluent of anion IC system was 5 mM sodium carbonate and 0.3 mM sodium hydroxide (made from $\geq 98\%$ pure sodium hydroxide, Sigma-Aldrich), and was used at a flow rate of 0.8 mL min^{-1} . The instruments were calibrated using standard cation and anion solutions (Dionex, CA, USA). The IC analysis results were evaluated in terms of the reproducibilities of peak retention times, peak heights, and the linearity of each calibration curve.

2.2.2 TOC and TN analysis

An aliquot of each sample was analyzed for TOC and TN contents using a high-sensitivity TOC/TN analyzer (TOC-V_{CPH} with a TNM-1unit, Shimadzu, Kyoto, Japan). The measurements were carried out using the total carbon (TC) and inorganic carbon

[Title Page](#)[Abstract](#)[Introduction](#)[Conclusions](#)[References](#)[Tables](#)[Figures](#)[◀](#)[▶](#)[◀](#)[▶](#)[Back](#)[Close](#)[Full Screen / Esc](#)[Printer-friendly Version](#)[Interactive Discussion](#)

(IC) method. The TC was determined by combusting the sample at 720 °C in a combustion tube filled with oxidation catalyst, which converted all carbon-containing components into CO₂. The CO₂ was detected by a non-dispersive infrared (NDIR) gas analyzer. The IC was defined as the carbon in carbonates and dissolved CO₂ in the sample. The carbonates were transformed into CO₂ by treating the sample with 25 % (by weight) phosphoric acid (H₃PO₄) in an IC reaction vessel. The CO₂ was then volatilized using a sparging procedure and detected by the NDIR analyzer. The TOC content was calculated by subtracting the inorganic carbon (IC) content from total carbon (TC) content. In the TN analysis the nitrogen-containing species were decomposed to NO in the combustion tube at 720 °C, then the sample was cooled and dehumidified using an electronic dehumidifier, and the NO was measured using a chemiluminescence gas analyzer. The total organic nitrogen (TON) was determined by subtracting the inorganic nitrogen (IN, which included ammonium and nitrate) content, quantified by IC, from the TN content. The samples were contained in well-sealed, pre-cleaned glass vials during analysis, and the instruments automatically withdrew a sample aliquot after piercing the vial seal. The calibrations were carried out using a potassium hydrogen phthalate standard for the TC determination, a sodium hydrogen carbonate for the IC determination, and potassium hydrogen phthalate and potassium nitrate standards for the TN determination.

2.2.3 HR-ToF-AMS analysis

Each filtered sample extract was aerosolized using argon and dehumidified using a diffusion dryer. The resulting aerosol particles were sampled into a HR-ToF-AMS instrument (Aerodyne Inc., Billerica, MA, USA) through an aerodynamic lens inlet, vaporized at ~ 600 °C, ionized by 70 eV electrons in an electron impact ionization chamber, and analyzed using the mass spectrometer. The HR-ToF-AMS analysis procedure for aqueous samples is described in detail elsewhere (Sun et al., 2011; Xu et al., 2013b). The HR-ToF-AMS was operated in the “V” and “W” ion optical modes alternatively, spending 2.5 min in each mode. In the V-mode the HR-ToF-AMS spent 6 s in the mass spectrum

J. Xu et al.

[Title Page](#)[Abstract](#)[Introduction](#)[Conclusions](#)[References](#)[Tables](#)[Figures](#)[◀](#)[▶](#)[◀](#)[▶](#)[Back](#)[Close](#)[Full Screen / Esc](#)[Printer-friendly Version](#)[Interactive Discussion](#)

(MS) mode and then 4 s in the particle time-of-flight (PToF) mode, then continuously repeated this 10 s cycle. In the W-mode the instrument used only the MS mode, with 6 s in each cycle. Between every two samples, purified waters ($> 18.2 \text{ M} \text{cm}^{-1}$, Millipore, USA) were analyzed in the same way to generate analytical blanks. Each sample was measured twice to check the reproducibility of the analysis. Elemental analyses were performed on high-resolution mass spectra (W-mode, with m/z up to 120), and these were used to determine the elemental ratios for oxygen to carbon (O/C), hydrogen to carbon (H/C), nitrogen to carbon (N/C), and organic mass-to-carbon (OM/OC) ratio of the DOM (Aiken et al., 2008). The elemental contributions of C, O, H, and N reported in this study are mass-based. The signals of H_2O^+ and CO^+ for organic compounds were not directly measured but scaled to that of CO_2^+ based on the evaluation of the H_2O^+ and CO^+ signal in the samples (Fig. S3): $\text{H}_2\text{O}^+ = 0.94 \times \text{CO}_2^+$, $\text{CO}^+ = 0.46 \times \text{CO}_2^+$.

Potential interferences on the CO_2^+ signals in the aerosol mass spectra caused by the presence of carbonate salts were evaluated by acidifying a sample (QSS1) to pH 4 using sulfuric acid and then analyzing the sample using the HR-ToF-AMS. Meanwhile, the volatility of the sample was investigated by a digitally controlled thermodenuder (TD) system. The sample was aerosolized and passed through a diffusion dryer, switched between the by-pass mode and TD mode every 5 min, and finally analyzed using the HR-ToF-AMS instrument. The TD system was programmed to cycle through 12 temperature steps (30, 50, 70, 100, 150, 200, 180, 130, 110, 88, 66, and then 40 °C). The design and use of the TD system have been described elsewhere (Fierz et al., 2007). The data were processed in a similar way as the normal HR-ToF-AMS data analysis, and the remaining particles calculated from the difference between the results of the TD mode and BP mode analysis were assumed to indicate the volatility of the aerosol species.

2.2.4 OC and EC analysis

The samples were analyzed for OC/EC using a Thermal/Optical Carbon Analyzer (DRI Model, 2001). The procedure used has been described in detail elsewhere (Cao et al.,

J. Xu et al.

Title Page

Abstract

Introduction

Conclusions

References

Tables

Figures

◀

▶

◀

▶

Back

Close

Full Screen / Esc

Printer-friendly Version

Interactive Discussion



2003). Briefly, the system heated the 0.526 cm² punched quartz filter aliquot gradually to 120 °C (fraction OC1), 250 °C (fraction OC2), 450 °C (fraction OC3), and 550 °C (fraction OC4) in a non-oxidizing helium atmosphere, and then to 550 °C (fraction EC1), 700 °C (fraction EC2), and 800 °C (fraction EC3) in an oxidizing atmosphere of 2 % oxygen in helium. The carbon evolved at each temperature was oxidized to CO₂, then reduced to methane (CH₄) and quantified using a flame ionization detector. Some of the organic carbon was pyrolyzed to form black carbon as temperature was increased in the helium atmosphere, resulting in the filter deposit becoming darker. This darkening was monitored by measuring the decrease in the reflectance of the sample using light at 633 nm from a He-Ne laser. The original black carbon and the pyrolyzed black carbon combusted after being exposed to the oxygen-containing atmosphere, and the reflectance increased. The amount of carbon measured after exposure to the oxygen-containing atmosphere until the reflectance reached its original value was reported as the optically detected pyrolyzed carbon (OPC). The eight fractions, OC1, OC2, OC3, OC4, EC1, EC2, EC3, and OPC were reported separately. OC was defined as OC1 + OC2 + OC3 + OC4 + OPC and EC was defined as EC1 + EC2 + EC3 – OPC in the IMPROCE protocol.

2.2.5 Determination of the water-soluble OM and water-insoluble OM concentrations

20 The mass concentrations of water-soluble OM (WSOM) and water-insoluble OM (WIOM), and the average OM/OC ratio for the organic matter (WSOM + WIOM) in PM_{2.5} are estimated using equations 1–3,

$$\text{WSOM} = \text{WSOC} \times \text{OM/OC}_{\text{WSOM}} \quad (1)$$

$$\text{WIOM} = (\text{OC} - \text{WSOC}) \times 1.3 \quad (2)$$

$$\text{OM/OC}_{\text{OM}} = (\text{WSOM} + \text{WIOM})/\text{OC} \quad (3)$$

[Title Page](#)[Abstract](#)[Introduction](#)[Conclusions](#)[References](#)[Tables](#)[Figures](#)[◀](#)[▶](#)[◀](#)
[Back](#)[▶](#)
[Close](#)[Full Screen / Esc](#)[Printer-friendly Version](#)[Interactive Discussion](#)

Where WSOC is the water-soluble organic carbon content in the filter extract measured by the TOC/TN analyzer, OM/OC_{WSOM} is the OM/OC ratio of the WSOM (determined from the HR-ToF-AMS measurement), OC is taken from the filter measurements using the thermo/optical carbon analyzer, the constant 1.3 in Eq. (2) is the estimated OM/OC for WIOM (Sun et al., 2011), and OM/OC_{OM} is the average OM/OC ratio of organic matter in PM_{2.5}.
5

2.2.6 Estimation of the secondary organic aerosol concentrations

The secondary organic carbon (SOC) content was estimated by determining the primary organic carbon (POC) content using EC as a tracer, and then subtracting the POC
10 from the measured total OC. The primary OA (POA) concentration was estimated using the POC as a tracer. Therefore, the SOA fraction was determined using OM/OC_{OM} and POA concentration. The equations used are shown below,

$$\text{POC} = (\text{OC}/\text{EC})_{\text{pri}} \times \text{EC} \quad (4)$$

$$\text{SOC} = \text{OC} - \text{POC} \quad (5)$$

$$15 \quad \text{POA} = \alpha \times \text{POC} \quad (6)$$

$$\text{SOA} = \text{OC} \times \text{OM}/\text{OC}_{\text{OM}} - \text{POA} \quad (7)$$

Where OC is the total OC. The POC can be calculated from the EC, and the estimated primary OC/EC ratio ((OC/EC)_{pri}) was based on the hypothesis that the primary OC and EC in ambient fine particles correlate strongly and stay at a constant ratio within
20 a geographical region. An OM/OC ratio (α) of 1.4 was used for the primary aerosol based on high resolution mass spectrometry at urban site of north China (1.2–1.6) (e.g., Xu et al., 2014b; Zhang, J. K. et al., 2014).

[Title Page](#)[Abstract](#)[Introduction](#)[Conclusions](#)[References](#)[Tables](#)[Figures](#)[Back](#)[Close](#)[Full Screen / Esc](#)[Printer-friendly Version](#)[Interactive Discussion](#)

3 Results and discussion

3.1 Chemical speciation of PM_{2.5}

The meteorological conditions during the measurement period were overall cold and humid. The air temperature (T) ranged from -5.9 to $14.3\text{ }^{\circ}\text{C}$, with an average of $4.2\text{ }^{\circ}\text{C}$, and the relative humidity (RH) ranged from 10.1 to 98.9 %, with an average of 65.2 % (Fig. 1a). Three-day air mass back trajectories originating at $\sim 100\text{ m a.g.l.}$ were acquired every 6 h during the sampling period and showed that 72 and 23 % of the air masses came from west and east of the sampling site, respectively (Fig. S1). Light precipitation occurred frequently between 11 July and 19 August (Fig. 1a) because of the topographic effect, but it was relatively dry from 19 August to 6 September, probably because of the occurrence of a different synoptic-scale weather pattern. The three-day average wind data also showed that the wind speed from west increased during the late part of the sampling period (Fig. S2). The wind direction changed diurnally, with moderate mountain wind (from the southeast at $\sim 2\text{ m s}^{-1}$) during the night and valley wind (from the north at $\sim 4\text{ m s}^{-1}$) during the day (Fig. 1b). The concentrations of various chemical species, including water soluble ionic species (WSIs), OC, EC, and TON, changed relatively little throughout the sampling period. No dust storm events were observed during the study even though the QSS is close to the desert regions.

The total mass concentrations of the measured species (WSIs + OC + EC + TON) throughout the sampling period were in the range of $1.8\text{--}8.0\text{ }\mu\text{g m}^{-3}$, and the average ($\pm 1\sigma$) was $3.7 \pm 1.9\text{ }\mu\text{g m}^{-3}$ (Fig. 2a), which were lower than that was measured in 2010 ($2.7\text{ }\mu\text{g m}^{-3}$ in 2012 vs. $5.4\text{ }\mu\text{g m}^{-3}$ in 2010 for the same WSIs in July and August) at the QSS (Xu et al., 2014a), probably because of the low frequency of dust storm events in 2012. Indeed, the mass concentration of calcium was significantly lower in 2012 ($0.27\text{ }\mu\text{g m}^{-3}$) than that in 2010 ($1.2\text{ }\mu\text{g m}^{-3}$). Overall, sulfate was the main contributor (on average 36.2 %) to the aerosol mass concentrations during the observation period (Fig. 2a), similar to previous observations in the northern QXP (Li et al., 2013; Xu et al., 2014a; Zhang, N. et al., 2014). The mass concentration of sulfate was also

Title Page

Abstract

Introduction

Conclusions

References

Tables

Figures

◀

▶

◀

▶

Back

Close

Full Screen / Esc

Printer-friendly Version

Interactive Discussion



lower in 2012 ($1.4 \mu\text{g m}^{-3}$) than that in 2010 ($2.7 \mu\text{g m}^{-3}$). The major cations (ammonium (10.1 %), calcium (6.6 %), sodium (1.5 %), magnesium (0.5 %), and potassium (0.3 %)) and anions (sulfate (36.2 %), nitrate (16.9 %), chloride (0.9 %)) together accounted for 44.5–88.3 % (mean 73.2 %) of the total aerosol mass. The ion balance, expressed as the ratio of the equivalent concentration (ueq m^{-3}) cation to that of anion (C/A), is shown in Fig. 2b. The mean C/A ratio was 0.97, which was close to 1, further indicating that the contribution of mineral dust was negligible since carbonate and bicarbonate were not measured in the IC analyses. The average EC concentration was $0.09 \mu\text{g m}^{-3}$ during the observation period, and its mean contribution to the total aerosol mass was 2.6 %. The average ($\pm 1\sigma$) concentration of OC and TON were $0.66 (\pm 0.43)$ and $0.24 (\pm 0.16) \mu\text{g m}^{-3}$, respectively. The OC and EC concentrations found in this study were lower than those found in the summer of 2010 at Qinghai Lake (1.6 and $0.4 \mu\text{g m}^{-3}$), which is also in the northern part of the QXP. The concentrations were different probably because Qinghai Lake is located at a lower elevation (3200 m.a.s.l.) (Li et al., 2013) than the QSS (4180 m.a.s.l.).

The correlation coefficients (r) between all of the chemical species are shown in Table 1, and the strong correlations ($r \geq 0.8$) are shown in bold. In general, strong correlation were found between the species in three groups, i.e., primary source (Ca^{2+} , Mg^{2+} , Na^+ , Cl^-), secondary ions (SO_4^{2-} , NO_3^- , NH_4^+ , K^+), and organics (OC, WSOC), indicating the major origination and aerosol process in the QSS region.

3.2 Chemically-resolved size distributions

The size distribution of all species is shown in Fig. 3, and the sum of the species presents a prominent accumulation mode and a coarse mode, peaking at MOUDI stage of 0.32–0.56 μm and 1.8–3.2 μm , respectively. In the accumulation mode, sulfate dominated (39.4 %) at the size range of 0.18–1 μm , with OC and EC accounting for 23.8 and 5.0 %, respectively, following by TON (9.4 %), NH_4^+ (7.9 %), NO_3^- (3.9 %), Cl^- (2.8 %), K^+ (1.3 %), and Ca^{2+} (0.6 %). However, OC dominated (36.3 %) the composition of

[Title Page](#)[Abstract](#)[Introduction](#)[Conclusions](#)[References](#)[Tables](#)[Figures](#)[◀](#)[▶](#)[◀](#)[▶](#)[Back](#)[Close](#)[Full Screen / Esc](#)[Printer-friendly Version](#)[Interactive Discussion](#)

particles smaller than 0.18 µm with sulfate contributing 25.5 %. At the coarse mode, nitrate was the main contributor, accounting for 22.8 % at the size range 1.8–5.6 µm, following by OC (16.6 %), sulfate (15.6 %), TON (11.6 %), Ca²⁺ (10.8 %), Cl⁻ (8.4 %), and EC (2.2 %); The rest of species totally accounted for 3.7 % at this size range. TON and OC were important contributors over the whole size range (0.056–18 µm).

The different behaviors of size distributions of different species suggested they had different sources and/or atmospheric transformation processes. No larger coarse mode (> 3 µm) aerosols were observed, suggesting that there was relatively little influence from locally produced soil particles. The species that were relatively abundant in the accumulation mode aerosols were mainly secondary species, such as ammonium, sulfate and OC, while the species that were relatively abundant in the coarse mode aerosols were mainly primary species, such as Ca²⁺, Na⁺, and Cl⁻. Nitrate was closely associated with dust particles as a result of its formation through the reactions of HNO₃ gas with carbonate salts (such as calcite and dolomite) (Sullivan et al., 2009) which could format Ca(NO₃)₂ and Mg(NO₃)₂ (Li and Shao, 2009). The equivalent balances analysis for species in the different size mode indicate that the accumulation mode particles was somewhat acidic (with the slope of [NH₄⁺ + Ca²⁺ + Mg⁺ + K⁺] vs. [SO₄²⁻ + NO₃⁻] of 0.6) and that the coarse mode particle was almost neutral (the slope was 0.999), as shown in Fig. 4. The acidic nature of the fine mode particles and the neutral nature of the coarse mode particles were similar with the results observed at Mt. Hua at 2009 (Wang et al., 2013). The acidic fine particle was probably an important factor retaining nitrate in coarse mode (Xue et al., 2014). The size of WSIs in these two modes were smaller than observed in other sites, such as in Hong Kong, where the accumulation mode was at 1–1.8 µm and the coarse mode was at 3.2–5.6 µm (Xue et al., 2014). The smaller mode size at the QSS was probably because of the lower specific humidity at QSS.

The OC and TON species in the coarse mode probably came from soil organic matter or were formed by the condensation of volatile organic gases on mineral dust. The EC and OC species reaching maximum concentration in the accumulation mode, con-

[Title Page](#)[Abstract](#)[Introduction](#)[Conclusions](#)[References](#)[Tables](#)[Figures](#)[◀](#)[▶](#)[◀](#)[▶](#)[Back](#)[Close](#)[Full Screen / Esc](#)[Printer-friendly Version](#)[Interactive Discussion](#)

The relationship between OC and EC concentrations can provide useful insights into the origin of carbonaceous aerosols, because particles from different sources have different OC/EC ratios. The correlation between the EC and OC concentrations at the QSS was statistically significant ($r^2 = 0.4$, $n = 19$), with the slope of 3.29 and the intercept of 0.23 (Fig. 5a and b). The OC/EC ratios ranged from 2.8 to 26.4 with the average of 7.6, which is higher than those observed from Chinese urban sites (1 to 4) (Cao et al., 2003). However, the OC/EC ratio at the QSS was similar to the ratios found at remote sites in Western China (Fig. S1) such as Qinghai Lake (6.0 ± 3.9 in $\text{PM}_{2.5}$) during the summer of 2010 (Li et al., 2013), Muztagh Ata Mountain (11.9 in total suspended particles) during the summers of 2004–2005 (Cao et al., 2009), and Akdala (12.2 in PM_{10}) during July 2004 and March 2005 (Qu et al., 2009). The high OC/EC ratios observed at the QSS suggest there was an important extra source of OC in the study region and/or secondary OC formation during the long range transport. The chemical characteristics of the organics can be further evaluated using the WSOC/OC ratio, which can be used to assess the aging of organic species. High WSOC/OC ratios (> 0.4) have been found in aged aerosols because a significant portion of the OC can be oxidized to WSOC (Ram et al., 2010). The WSOC and OC concentrations in the QSS were strongly positively correlated ($r^2 = 0.99$) with the slope of 0.79. This slope is higher than those in Chinese urban sites (0.3–0.6) (Pathak et al., 2011) and at remote sites in Western China, such as Qinghai Lake (0.42) during the summer of 2012 (Li et al., 2013) and Himalayas (0.26–0.51) (Rengarajan et al., 2007; Ram et al., 2010; Shrestha et al., 2010). The high WSOC/OC ratios that were found in the aerosol samples from the QSS can be regarded as a solid evidence of the formation of SOA because of its high solubility in water.

3.4 Spectra characteristics of the WSOM

The average MS for WSOM in PM_{2.5} samples is shown in Fig. 6. The major spectral features are the extremely high mass fraction of m/z 44 (f_{44}) (mainly CO₂⁺, 94.6 %), m/z 18 (H₂O⁺), and m/z 28 (CO⁺). The f_{44} peaks were almost identical (~ 20 %) in all filter samples, and in two samples, QSS3 and QSS18, the contributions of f_{44} peaks were particularly high, at 27.4 and 27.3 %, respectively. It has previously been suggested that CO₂⁺ ion in the HR-ToF-AMS MS is typically associated with the presence of carboxylic acids (Takegawa et al., 2007), which can be oxidation products of organic species through heterogeneous and homogeneous chemical processes (fragmentation) (Jimenez et al., 2009). This can be supported by the low intensity fragments at the high m/z range ($m/z > 50$), which were probably caused by the fragmentation of organic species during oxidation and conversion into small organic acids (increasing f_{44}). The similarities between the mass spectra of the acidified and untreated QSS1 sample ($r^2 = 0.98$; Fig. S4) ruled out the potential influence of carbonate salts on the intensity of the CO₂⁺ peak. The O/C ratio, an oxidation degree index, has a mean value of 1.16 and a range of 0.93–1.66 (Fig. 6a). The mean OM/OC ratio for our filter samples was 2.75, which contrasts strongly with the range of 1.6–2.2 found in other studies, indicating that secondary organic aerosol made important contributions to the aerosols in our study. The H/C ratio was also relatively high, at 1.89. The high O/C and H/C ratios were caused not only by the high contribution of CO₂⁺ ions but also by the high contribution from H₂O⁺, which can be produced by the fragmentation of acidic species. Carbon oxidation state (OSc) values are more robust and less variable than measured H/C and O/C ratios, so we calculated the OSc values ($2 \times \text{O/C} - \text{H/C}$). The mean OSc for the filter samples was 0.4 ranging between 0.1 and 1.2, similar to the OSc values of diacids and multifunctional acids (Canagaratna et al., 2014). The elemental composition of the WSOM in the filter samples was C (36 %), O (56 %), H (6 %), and N (2 %). The mass spectrum was composed of H_yO₁⁺ (25 %), C_xH_yO₁⁺ (22 %), C_xH_yO₂⁺ (23 %), and C_xH_y⁺ (25 %) ions, indicating that oxygenated functional groups were predominant

Title Page

Abstract

Introduction

Conclusions

References

Tables

Figures

◀

▶

◀

▶

Back

Close

Full Screen / Esc

Printer-friendly Version

Interactive Discussion



in the WSOM. The high contribution from H_yO_1^+ ions could be generated from diacids and alcohols (Canagaratna et al., 2014).

The high oxidation state of organics at the remote area of northern QXP has been suggested in a previous study at Qinghai Lake in 2010 based on the diagnostic ratios of $\text{C}_{18:1}/\text{C}_{18:0}$ and Bap/Bep (Li et al., 2013). We sought further evidence for the high oxidation state of organics in our samples by checking the volatility of OC, which normally has a reverse relationship with the degree of oxidation (Huffman et al., 2009). The OC mass fractions that evaporated at different temperature step were 12 % at 120 °C (OC1), 26 % at 250 °C (OC2), 39 % at 450 °C (OC3), and 23 % at 550 °C (OC4), respectively. The large fractions of OC at high temperature suggested its low volatility. Indeed, the volatility measurements performed using the TD system on the QSS1 sample indicated that the organic species were less volatile than ammonium and nitrate and more volatile than sulfate (Fig. 7a). However the remaining fraction of organics was higher than sulfate at 180–200 °C (Fig. 7b). The volatility distribution of the WSOM of the QSS1 sample were similar to that of LV-OOA in samples from urban sites (Huffman et al., 2009).

The MS showed that the QSS organic species were more oxidized than the oxygenated organic aerosol factors (e.g., LV-OOA, which had an O/C ratio of 0.5–1) observed at urban sites, determined using positive matrix factorization analysis (Aiken et al., 2008; Ng et al., 2010). The higher level of oxidation of organic species in our samples was probably caused by chemical processes such as photo-chemistry and/or aqueous process in cloud and particle water because of the stronger solar radiation at high elevation mountain area and the higher humidity during the upslope transport of air mass from the lowlands. The highly oxidized MS is very similar to that in study of Lee et al. (2012) ($r^2 = 0.87$, Fig. S5), which oxidized the field filter samples collected in a mountain site in the laboratory in a photochemical reactor. The potentially strong oxidizing environment at the QSS was another important factor in producing the highly oxidized organic species. For example, the photochemical reactions on snow/ice are

Title Page

Abstract

Introduction

Conclusions

References

Tables

Figures

◀

▶

◀

▶

Back

Close

Full Screen / Esc

Printer-friendly Version

Interactive Discussion



suspected to the release of reactive gaseous species, including H₂O₂, HONO, and further OH (Grannas et al., 2007).

3.5 Estimation of secondary organic aerosol concentrations

The EC-tracer method estimates the SOC concentration from the relationship of POC and EC has been widely used, although the uncertainty may arise due to the fixed (OC/EC)_{primary} ratio. For determining the (OC/EC)_{primary} ratio, the minimum OC/EC value is usually used for the remote site rather than the slope of linear regression between OC and EC, which may provide over-estimation of SOA because of the use of higher OC/EC ratio resulting from already formed secondary organic aerosols. In addition, the fixed (OC/EC)_{primary} ratio is used in this study because the low time resolution of samples (3 days) which could be the mixture of POA and SOA. The primary OC/EC ratio of 2.77 used in this study, is higher than those observed from urban sites (where OC/EC ratio < 1 had been found) (Plaza et al., 2006; Huang et al., 2013); This is partially because the measured OC concentrations are generally much higher than EC concentrations during the summer, especially for the particles after long-range transport. However, this value is similar to the value of 2.0 that is commonly used to estimate the presence of SOA (Chow et al., 1996) and the typical minimum OC/EC ratio that has been used for estimation of SOA concentration at remote sites such as Mount Heng (2.2) (Zhou et al., 2012) and Mount Tai (2.19) (Wang et al., 2012) in China.

The average concentration of SOC at the QSS during the summer was $0.38 \pm 0.36 \mu\text{g m}^{-3}$, on average accounting for 52.3 % (0–90 %) of the total OC (Fig. 8a and b). The average concentration of SOA was $1.19 \pm 0.87 \mu\text{g m}^{-3}$, on average accounting for 75.3 % (46.4–96.4 %) of the total OA (Fig. 8c and d). These results indicate that secondary aerosols were dominant at the QSS during the summer. The SOC and SOA contributed relatively small to the aerosols during the late sampling period, and this is consistent with less chances of aqueous processing during this period. The SOC contribution at the QSS is consistent with those (36–52 %) at Himalayas during summer. For example, Ram et al. (2008) found, using the EC-tracer method, that SOC

Title Page

Abstract

Introduction

Conclusions

References

Tables

Figures

◀

▶

◀

▶

Back

Close

Full Screen / Esc

Printer-friendly Version

Interactive Discussion



contributed 52 % of the aerosols at Manora Peak during summer. The estimated SOC contribution is also consistent the results at Mount Heng (53.9 % of the total OC) and at Mount Tai (57.3 and 71.2 % of total OC in spring and summer, respectively) (Wang et al., 2012; Zhou et al., 2012).

5 4 Conclusions

An intensive study was conducted at the QSS in the northern part of the QXP, to characterize the chemical compositions of $\text{PM}_{2.5}$ during the summer of 2012 because of the strong exchange between boundary layer and free troposphere during this period. The average mass concentration of the total chemicals including WSI (Na^+ , NH_4^+ , K^+ , Ca^{2+} , Mg^{2+} , Cl^- , NO_3^- , and SO_4^{2-}), OC, EC, and TON, was $3.7 \pm 1.9 \mu\text{g m}^{-3}$. The main contributor to the aerosol was SO_4^{2-} (36.2 % of the total), followed by OC (17.8 %), NO_3^- (16.9 %), NH_4^+ (10.1 %), Ca^{2+} (6.6 %), TON (6.4 %), and EC (2.6 %). The size distribution of the particles presented a bimodal distribution with a prominent accumulation mode (0.32–0.56 μm) and a coarse mode (1.8–3.2 μm). Sulfate, OC, and EC dominated the accumulation mode (contributing ~70 %), while nitrate was the main contributor to the coarse mode (contributing 22.8 %), followed by OC (16.6 %), sulfate (15.6 %), TON (11.6 %), Ca^{2+} (10.8 %), Cl^- (8.4 %), and EC (2.2 %). Stoichiometry analysis indicated that particles in sub-micrometer size range were acidic and coarse particles were mostly neutral. The OC was dominated by WSOC (contributing 79 %), suggesting the important contribution of secondary OC. The WSOM was chemically characterized using HR-ToF-AMS, which showed highly oxygenated organic species were major contributors to the WSOM. The average MS of WSOM was dominated by H_yO_1^+ (24 %), $\text{C}_x\text{H}_y\text{O}_1^+$ (22 %), $\text{C}_x\text{H}_y\text{O}_2^+$ (22 %), and C_xH_y^+ (26 %), and the O/C and OM/OC ratios were 1.16 and 2.75, respectively. These results suggest that the organic species became more oxidized during the long-range transport and/or at the local environment at the QSS through chemical processing, such as the aqueous process during

[Title Page](#)[Abstract](#)[Introduction](#)[Conclusions](#)[References](#)[Tables](#)[Figures](#)[◀](#)[▶](#)[Back](#)[Close](#)[Full Screen / Esc](#)[Printer-friendly Version](#)[Interactive Discussion](#)

the upslope transport of the aerosol from lowland to elevated mountain areas. The estimated SOA on average accounted for 75.3 % (range 46.4–96.4 %) of the aerosol mass, which is higher than those reported from Himalayas. Our results could also be useful for a better understanding of the chemical content of snow and glaciers around the QSS.

**The Supplement related to this article is available online at
doi:10.5194/acpd-15-1307-2015-supplement.**

Acknowledgements. This research was supported by grants from the Hundred Talents Program of Chinese Academy of Sciences, the Science Fund for Creative Research Groups of the National Natural Science Foundation of China (NSFC) (41121001) and the Scientific Research Foundation of the Key Laboratory of Cryospheric Sciences (SKLCS-ZZ-2013-01-04).

References

- Aiken, A. C., DeCarlo, P. F., Kroll, J. H., Worsnop, D. R., Huffman, J. A., Docherty, K. S., Ulbrich, I. M., Mohr, C., Kimmel, J. R., Sueper, D., Sun, Y., Zhang, Q., Trimborn, A., Northway, M., Ziemann, P. J., Canagaratna, M. R., Onasch, T. B., Alfarra, M. R., Prevot, A. S. H., Dommen, J., Duplissy, J., Metzger, A., Baltensperger, U., and Jimenez, J. L.: O/C and OM/OC ratios of primary, secondary, and ambient organic aerosols with high-resolution time-of-flight aerosol mass spectrometry, Environ. Sci. Technol., 42, 4478–4485, doi:10.1021/es703009q, 2008.
- Bonasoni, P., Laj, P., Angelini, F., Arduini, J., Bonafè, U., Calzolari, F., Cristofanelli, P., Decesari, S., Facchini, M. C., Fuzzi, S., Gobbi, G. P., Maione, M., Marinoni, A., Petzold, A., Roccato, F., Roger, J. C., Sellegri, K., Sprenger, M., Venzac, H., Verza, G. P., Villani, P., and Vuillermoz, E.: The abc-pyramid atmospheric research observatory in himalaya for aerosol, ozone and halocarbon measurements, Sci. Total. Environ., 391, 252–261, doi:10.1016/j.scitotenv.2007.10.024, 2008.

J. Xu et al.

[Title Page](#)[Abstract](#)[Introduction](#)[Conclusions](#)[References](#)[Tables](#)[Figures](#)[◀](#)[▶](#)[Back](#)[Close](#)[Full Screen / Esc](#)[Printer-friendly Version](#)[Interactive Discussion](#)

Canagaratna, M. R., Jimenez, J. L., Kroll, J. H., Chen, Q., Kessler, S. H., Massoli, P., Hildebrandt Ruiz, L., Fortner, E., Williams, L. R., Wilson, K. R., Surratt, J. D., Donahue, N. M., Jayne, J. T., and Worsnop, D. R.: Elemental ratio measurements of organic compounds using aerosol mass spectrometry: characterization, improved calibration, and implications, *Atmos. Chem. Phys. Discuss.*, 14, 19791–19835, doi:10.5194/acpd-14-19791-2014, 2014.

Cao, J. J., Lee, S. C., Ho, K. F., Zhang, X. Y., Zou, S. C., Fung, K., Chow, J. C., and Watson, J. G.: Characteristics of carbonaceous aerosol in pearl river delta region, china during 2001 winter period, *Atmos. Environ.*, 37, 1451–1460, doi:10.1016/S1352-2310(02)01002-6, 2003.

Cao, J. J., Xu, B. Q., He, J. Q., Liu, X. Q., Han, Y. M., Wang, G. H., and Zhu, C. S.: Concentrations, seasonal variations, and transport of carbonaceous aerosols at a remote mountainous region in western china, *Atmos. Environ.*, 43, 4444–4452, doi:10.1016/j.atmosenv.2009.06.023, 2009.

Carrico, C. M., Bergin, M. H., Shrestha, A. B., Dibb, J. E., Gomes, L., and Harris, J. M.: The importance of carbon and mineral dust to seasonal aerosol properties in the nepal himalaya, *Atmos. Environ.*, 37, 2811–2824, doi:10.1016/s1352-2310(03)00197-3, 2003.

Chow, J. C., Watson, J. G., Lu, Z., Lowenthal, D. H., Frazier, C. A., Solomon, P. A., Thuillier, R. H., and Magliano, K.: Descriptive analysis of PM_{2.5} and PM₁₀ at regionally representative locations during sjvaqs/auspex, *Atmos. Environ.*, 30, 2079–2112, doi:10.1016/1352-2310(95)00402-5, 1996.

Cong, Z., Kang, S., Liu, X., and Wang, G.: Elemental composition of aerosol in the nam co region, tibetan plateau, during summer monsoon season, *Atmos. Environ.*, 41, 1180–1187, doi:10.1016/j.atmosenv.2006.09.046, 2007.

Decesari, S., Facchini, M. C., Carbone, C., Giulianelli, L., Rinaldi, M., Finessi, E., Fuzzi, S., Marignoni, A., Cristofanelli, P., Duchi, R., Bonasoni, P., Vuillermoz, E., Cozic, J., Jaffrezo, J. L., and Laj, P.: Chemical composition of PM₁₀ and PM₁ at the high-altitude Himalayan station Nepal Climate Observatory-Pyramid (NCO-P) (5079 m a.s.l.), *Atmos. Chem. Phys.*, 10, 4583–4596, doi:10.5194/acp-10-4583-2010, 2010.

Engling, G., Zhang, Y.-N., Chan, C.-Y., Sang, X.-F., Lin, M., Ho, K.-F., Li, Y.-S., Lin, C.-Y., and Lee, J. J.: Characterization and sources of aerosol particles over the southeastern tibetan plateau during the southeast asia biomass-burning season, *Tellus B*, 63, 117–128, doi:10.1111/j.1600-0889.2010.00512.x, 2011.

Fierz, M., Vernooij, M. G. C., and Burtscher, H.: An improved low-flow thermodenuder, *J. Aerosol Sci.*, 38, 1163–1168, doi:10.1016/j.jaerosci.2007.08.006, 2007.

Title Page

Abstract

Introduction

Conclusions

References

Tables

Figures

◀

▶

◀

▶

Back

Close

Full Screen / Esc

Printer-friendly Version

Interactive Discussion



Grannas, A. M., Jones, A. E., Dibb, J., Ammann, M., Anastasio, C., Beine, H. J., Bergin, M., Bottenheim, J., Boxe, C. S., Carver, G., Chen, G., Crawford, J. H., Dominé, F., Frey, M. M., Guzmán, M. I., Heard, D. E., Helmig, D., Hoffmann, M. R., Honrath, R. E., Huey, L. G., Hutterli, M., Jacobi, H. W., Klán, P., Lefer, B., McConnell, J., Plane, J., Sander, R., Savarino, J., Shepson, P. B., Simpson, W. R., Sodeau, J. R., von Glasow, R., Weller, R., Wolff, E. W., and Zhu, T.: An overview of snow photochemistry: evidence, mechanisms and impacts, *Atmos. Chem. Phys.*, 7, 4329–4373, doi:10.5194/acp-7-4329-2007, 2007.

Hegde, P. and Kawamura, K.: Seasonal variations of water-soluble organic carbon, dicarboxylic acids, ketocarboxylic acids, and α -dicarbonyls in Central Himalayan aerosols, *Atmos. Chem. Phys.*, 12, 6645–6665, doi:10.5194/acp-12-6645-2012, 2012.

Huang, X.-F., Xue, L., Tian, X.-D., Shao, W.-W., Sun, T.-L., Gong, Z.-H., Ju, W.-W., Jiang, B., Hu, M., and He, L.-Y.: Highly time-resolved carbonaceous aerosol characterization in yangtze river delta of china: Composition, mixing state and secondary formation, *Atmos. Environ.*, 64, 200–207, doi:10.1016/j.atmosenv.2012.09.059, 2013.

Huffman, J. A., Docherty, K. S., Aiken, A. C., Cubison, M. J., Ulbrich, I. M., DeCarlo, P. F., Sueper, D., Jayne, J. T., Worsnop, D. R., Ziemann, P. J., and Jimenez, J. L.: Chemically-resolved aerosol volatility measurements from two megacity field studies, *Atmos. Chem. Phys.*, 9, 7161–7182, doi:10.5194/acp-9-7161-2009, 2009.

Jimenez, J. L., Canagaratna, M. R., Donahue, N. M., Prevot, A. S. H., Zhang, Q., Kroll, J. H., DeCarlo, P. F., Allan, J. D., Coe, H., Ng, N. L., Aiken, A. C., Docherty, K. S., Ulbrich, I. M., Grieshop, A. P., Robinson, A. L., Duplissy, J., Smith, J. D., Wilson, K. R., Lanz, V. A., Hueglin, C., Sun, Y. L., Tian, J., Laaksonen, A., Raatikainen, T., Rautiainen, J., Vaattovaara, P., Ehn, M., Kulmala, M., Tomlinson, J. M., Collins, D. R., Cubison, M. J., Dunlea, J., Huffman, J. A., Onasch, T. B., Alfarra, M. R., Williams, P. I., Bower, K., Kondo, Y., Schneider, J., Drewnick, F., Borrmann, S., Weimer, S., Demerjian, K., Salcedo, D., Cottrell, L., Griffin, R., Takami, A., Miyoshi, T., Hatakeyama, S., Shimono, A., Sun, J. Y., Zhang, Y. M., Dzepina, K., Kimmel, J. R., Sueper, D., Jayne, J. T., Herndon, S. C., Trimborn, A. M., Williams, L. R., Wood, E. C., Middlebrook, A. M., Kolb, C. E., Baltensperger, U., and Worsnop, D. R.: Evolution of organic aerosols in the atmosphere, *Science*, 326, 1525–1529, doi:10.1126/science.1180353, 2009.

Kanakidou, M., Seinfeld, J. H., Pandis, S. N., Barnes, I., Dentener, F. J., Facchini, M. C., Van Dingenen, R., Ervens, B., Nenes, A., Nielsen, C. J., Swietlicki, E., Putaud, J. P., Balkanski, Y., Fuzzi, S., Horth, J., Moortgat, G. K., Winterhalter, R., Myhre, C. E. L., Tsigaridis, K.,

Insights into the chemical composition of summertime PM_{2.5}

J. Xu et al.

[Title Page](#)

[Abstract](#)

[Introduction](#)

[Conclusions](#)

[References](#)

[Tables](#)

[Figures](#)



[Full Screen / Esc](#)

[Printer-friendly Version](#)

[Interactive Discussion](#)



- Vignati, E., Stephanou, E. G., and Wilson, J.: Organic aerosol and global climate modelling: a review, *Atmos. Chem. Phys.*, 5, 1053–1123, doi:10.5194/acp-5-1053-2005, 2005.
- Lee, A. K. Y., Hayden, K. L., Herckes, P., Leaitch, W. R., Liggio, J., Macdonald, A. M., and Abbatt, J. P. D.: Characterization of aerosol and cloud water at a mountain site during WACS 2010: secondary organic aerosol formation through oxidative cloud processing, *Atmos. Chem. Phys.*, 12, 7103–7116, doi:10.5194/acp-12-7103-2012, 2012.
- Li, J. J., Wang, G. H., Wang, X. M., Cao, J. J., Sun, T., Cheng, C. L., Meng, J. J., Hu, T. F., and Liu, S. X.: Abundance, composition and source of atmospheric PM_{2.5} at a remote site in the Tibetan Plateau, China, *Tellus B*, 65, 1–16, doi:10.3402/tellusb.v65i0.20281, 2013.
- Li, S.-M., Tang, J., Xue, H., and Toom-Sauntry, D.: Size distribution and estimated optical properties of carbonate, water soluble organic carbon, and sulfate in aerosols at a remote high altitude site in Western China, *Geophys. Res. Lett.*, 27, 1107–1110, doi:10.1029/1999GL010929, 2000.
- Li, W. J. and Shao, L. Y.: Observation of nitrate coatings on atmospheric mineral dust particles, *Atmos. Chem. Phys.*, 9, 1863–1871, doi:10.5194/acp-9-1863-2009, 2009.
- Meng, J., Wang, G., Li, J., Cheng, C., and Cao, J.: Atmospheric oxalic acid and related secondary organic aerosols in qinghai lake, a continental background site in Tibet Plateau, *Atmos. Environ.*, 79, 582–589, doi:10.1016/j.atmosenv.2013.07.024, 2013.
- Ng, N. L., Canagaratna, M. R., Zhang, Q., Jimenez, J. L., Tian, J., Ulbrich, I. M., Kroll, J. H., Docherty, K. S., Chhabra, P. S., Bahreini, R., Murphy, S. M., Seinfeld, J. H., Hildebrandt, L., Donahue, N. M., DeCarlo, P. F., Lanz, V. A., Prévôt, A. S. H., Dinar, E., Rudich, Y., and Worsnop, D. R.: Organic aerosol components observed in Northern Hemispheric datasets from Aerosol Mass Spectrometry, *Atmos. Chem. Phys.*, 10, 4625–4641, doi:10.5194/acp-10-4625-2010, 2010.
- Pathak, R. K., Wang, T., Ho, K. F., and Lee, S. C.: Characteristics of summertime pm2.5 organic and elemental carbon in four major chinese cities: Implications of high acidity for water-soluble organic carbon (WSOC), *Atmos. Environ.*, 45, 318–325, doi:10.1016/j.atmosenv.2010.10.021, 2011.
- Plaza, J., Gómez-Moreno, F. J., Núñez, L., Pujadas, M., and Artíñano, B.: Estimation of secondary organic aerosol formation from semi-continuous OC–EC measurements in a madrid suburban area, *Atmos. Environ.*, 40, 1134–1147, doi:10.1016/j.atmosenv.2005.11.007, 2006.

Insights into the chemical composition of summertime PM_{2.5}

J. Xu et al.

[Title Page](#)[Abstract](#)[Introduction](#)[Conclusions](#)[References](#)[Tables](#)[Figures](#)[Back](#)[Close](#)[Full Screen / Esc](#)[Printer-friendly Version](#)[Interactive Discussion](#)

Title Page	
Abstract	Introduction
Conclusions	References
Tables	Figures
	
Back	Close
Full Screen / Esc	
Printer-friendly Version	
Interactive Discussion	



Qu, W.-J., Zhang, X.-Y., Arimoto, R., Wang, Y.-Q., Wang, D., Sheng, L.-F., and Fu, G.: Aerosol background at two remote cawnet sites in Western China, *Sci. Total Environ.*, 407, 3518–3529, doi:10.1016/j.scitotenv.2009.02.012, 2009.

Ram, K., Sarin, M. M., and Hegde, P.: Atmospheric abundances of primary and secondary carbonaceous species at two high-altitude sites in India: Sources and temporal variability, *Atmos. Environ.*, 42, 6785–6796, doi:10.1016/j.atmosenv.2008.05.031, 2008.

Ram, K., Sarin, M. M., and Hegde, P.: Long-term record of aerosol optical properties and chemical composition from a high-altitude site (Manora Peak) in Central Himalaya, *Atmos. Chem. Phys.*, 10, 11791–11803, doi:10.5194/acp-10-11791-2010, 2010.

Rengarajan, R., Sarin, M. M., and Sudheer, A. K.: Carbonaceous and inorganic species in atmospheric aerosols during wintertime over urban and high-altitude sites in north India, *J. Geophys. Res.*, 112, D21307, doi:10.1029/2006jd008150, 2007.

Sang, X., Zhang, Z., Chan, C., and Engling, G.: Source categories and contribution of biomass smoke to organic aerosol over the southeastern Tibetan plateau, *Atmos. Environ.*, 78, 113–123, doi:10.1016/j.atmosenv.2012.12.012, 2013.

Shrestha, P., Barros, A. P., and Khlystov, A.: Chemical composition and aerosol size distribution of the middle mountain range in the Nepal Himalayas during the 2009 pre-monsoon season, *Atmos. Chem. Phys.*, 10, 11605–11621, doi:10.5194/acp-10-11605-2010, 2010.

Sullivan, R. C., Moore, M. J. K., Petters, M. D., Kreidenweis, S. M., Roberts, G. C., and Prather, K. A.: Timescale for hygroscopic conversion of calcite mineral particles through heterogeneous reaction with nitric acid, *Phys. Chem. Chem. Phys.*, 11, 7826–7837, doi:10.1039/b904217b, 2009.

Sun, Y., Zhang, Q., Macdonald, A. M., Hayden, K., Li, S. M., Liggio, J., Liu, P. S. K., Anlauf, K. G., Leaitch, W. R., Steffen, A., Cubison, M., Worsnop, D. R., van Donkelaar, A., and Martin, R. V.: Size-resolved aerosol chemistry on Whistler Mountain, Canada with a high-resolution aerosol mass spectrometer during INTEX-B, *Atmos. Chem. Phys.*, 9, 3095–3111, doi:10.5194/acp-9-3095-2009, 2009.

Sun, Y., Zhang, Q., Zheng, M., Ding, X., Edgerton, E. S., and Wang, X.: Characterization and source apportionment of water-soluble organic matter in atmospheric fine particles (PM_{2.5}) with high-resolution aerosol mass spectrometry and GC–MS, *Environ. Sci. Technol.*, 45, 4854–4861, doi:10.1021/es200162h, 2011.

Takegawa, N., Miyakawa, T., Kawamura, K., and Kondo, Y.: Contribution of selected dicarboxylic and ω -oxocarboxylic acids in ambient aerosol to the m/z 44 signal of an aerodyne aerosol

- mass spectrometer, *Aerosol Sci. Tech.*, 41, 418–437, doi:10.1080/02786820701203215, 2007.
- Ulbrich, I. M., Canagaratna, M. R., Zhang, Q., Worsnop, D. R., and Jimenez, J. L.: Interpretation of organic components from Positive Matrix Factorization of aerosol mass spectrometric data, *Atmos. Chem. Phys.*, 9, 2891–2918, doi:10.5194/acp-9-2891-2009, 2009.
- Wang, G. H., Zhou, B. H., Cheng, C. L., Cao, J. J., Li, J. J., Meng, J. J., Tao, J., Zhang, R. J., and Fu, P. Q.: Impact of Gobi desert dust on aerosol chemistry of Xi'an, inland China during spring 2009: differences in composition and size distribution between the urban ground surface and the mountain atmosphere, *Atmos. Chem. Phys.*, 13, 819–835, doi:10.5194/acp-13-819-2013, 2013.
- Wang, Z., Wang, T., Guo, J., Gao, R., Xue, L., Zhang, J., Zhou, Y., Zhou, X., Zhang, Q., and Wang, W.: Formation of secondary organic carbon and cloud impact on carbonaceous aerosols at Mount Tai, North China, *Atmos. Environ.*, 46, 516–527, doi:10.1016/j.atmosenv.2011.08.019, 2012.
- Xu, J., Wang, Z., Yu, G., Sun, W., Qin, X., Ren, J., and Qin, D.: Seasonal and diurnal variations in aerosol concentrations at a high-altitude site on the northern boundary of Qinghai-Xizang Plateau, *Atmos. Res.*, 120–121, 240–248, doi:10.1016/j.atmosres.2012.08.022, 2013a.
- Xu, J., Zhang, Q., Li, X., Ge, X., Xiao, C., Ren, J., and Qin, D.: Dissolved organic matter and inorganic ions in a central himalayan glacier – insights into chemical composition and atmospheric sources, *Environ. Sci. Technol.*, 47, 6181–6188, doi:10.1021/es4009882, 2013b.
- Xu, J., Wang, Z., Yu, G., Qin, X., Ren, J., and Qin, D.: Characteristics of water soluble ionic species in fine particles from a high altitude site on the northern boundary of ti-betan plateau: Mixture of mineral dust and anthropogenic aerosol, *Atmos. Res.*, 143, 43–56, doi:10.1016/j.atmosres.2014.01.018, 2014a.
- Xu, J., Zhang, Q., Chen, M., Ge, X., Ren, J., and Qin, D.: Chemical composition, sources, and processes of urban aerosols during summertime in northwest China: insights from high-resolution aerosol mass spectrometry, *Atmos. Chem. Phys.*, 14, 12593–12611, doi:10.5194/acp-14-12593-2014, 2014.
- Xue, J., Yuan, Z., Lau, A. K. H., and Yu, J. Z.: Insights into factors affecting nitrate in PM_{2.5} in a polluted high NO_x environment through hourly observations and size distribution measurements, *J. Geophys. Res.-Atmos.*, 119, 4888–4902, doi:10.1002/2013JD021108, 2014.
- Yao, T., Thompson, L. G., Mosbrugger, V., Zhang, F., Ma, Y., Luo, T., Xu, B., Yang, X., Joswiak, D. R., Wang, W., Joswiak, M. E., Devkota, L. P., Tayal, S., Jilani, R., and Fayziev, R.: 30

[Title Page](#)[Abstract](#)[Introduction](#)[Conclusions](#)[References](#)[Tables](#)[Figures](#)[◀](#)[▶](#)[◀](#)[▶](#)[Back](#)[Close](#)[Full Screen / Esc](#)[Printer-friendly Version](#)[Interactive Discussion](#)

Third pole environment (tpe), Environ. Dev., 3, 52–64, doi:10.1016/j.envdev.2012.04.002, 2012.

5 Yu, H. and Yu, J. Z.: Modal characteristics of elemental and organic carbon in an urban location in Guangzhou, China, Aerosol Sci. Tech., 43, 1108–1118, doi:10.1080/02786820903196878, 2009.

Zhang, J. K., Sun, Y., Liu, Z. R., Ji, D. S., Hu, B., Liu, Q., and Wang, Y. S.: Characterization of submicron aerosols during a month of serious pollution in Beijing, 2013, Atmos. Chem. Phys., 14, 2887–2903, doi:10.5194/acp-14-2887-2014, 2014.

10 Zhang, N., Cao, J., Liu, S., Zhao, Z., Xu, H., and Xiao, S.: Chemical composition and sources of PM_{2.5} and tsp collected at Qinghai Lake during summertime, Atmos. Res., 138, 213–222, doi:10.1016/j.atmosres.2013.11.016, 2014.

15 Zhang, Q., Jimenez, J. L., Canagaratna, M. R., Allan, J. D., Coe, H., Ulbrich, I., Alfarra, M. R., Takami, A., Middlebrook, A. M., Sun, Y. L., Dzepina, K., Dunlea, E., Docherty, K., DeCarlo, P. F., Salcedo, D., Onasch, T., Jayne, J. T., Miyoshi, T., Shimono, A., Hatakeyama, S., Takegawa, N., Kondo, Y., Schneider, J., Drewnick, F., Borrmann, S., Weimer, S., Demerjian, K., Williams, P., Bower, K., Bahreini, R., Cottrell, L., Griffin, R. J., Rautiainen, J., Sun, J. Y., Zhang, Y. M., and Worsnop, D. R.: Ubiquity and dominance of oxygenated species in organic aerosols in anthropogenically-influenced Northern Hemisphere midlatitudes, Geophys. Res. Lett., 34, L13801, doi:10.1029/2007gl029979, 2007.

20 Zhang, Q., Jimenez, J. L., Canagaratna, M. R., Ulbrich, I. M., Ng, N. L., Worsnop, D. R., and Sun, Y.: Understanding atmospheric organic aerosols via factor analysis of aerosol mass spectrometry: a review, Anal. Bioanal. Chem., 401, 3045–3067, doi:10.1007/s00216-011-5355-y, 2011.

25 Zhao, Z., Cao, J., Shen, Z., Xu, B., Zhu, C., Chen, L. W. A., Su, X., Liu, S., Han, Y., Wang, G., and Ho, K.: Aerosol particles at a high-altitude site on the Southeast Tibetan Plateau, China: implications for pollution transport from south asia, J. Geophys. Res., 118, 11360–11375, doi:10.1002/jgrd.50599, 2013.

30 Zhou, S., Wang, Z., Gao, R., Xue, L., Yuan, C., Wang, T., Gao, X., Wang, X., Nie, W., Xu, Z., Zhang, Q., and Wang, W.: Formation of secondary organic carbon and long-range transport of carbonaceous aerosols at Mount Heng in South China, Atmos. Environ., 63, 203–212, doi:10.1016/j.atmosenv.2012.09.021, 2012.

Insights into the chemical composition of summertime PM_{2.5}

J. Xu et al.

[Title Page](#)

[Abstract](#)

[Introduction](#)

[Conclusions](#)

[References](#)

[Tables](#)

[Figures](#)



[◀](#)

[▶](#)

[Back](#)

[Close](#)

[Full Screen / Esc](#)

[Printer-friendly Version](#)

[Interactive Discussion](#)



Table 1. Correlation coefficients (Pearson's r) between the water soluble inorganic ions, organic carbon (OC), elemental carbon (EC), water soluble organic carbon (WSOC), and total water soluble nitrogen (TON) concentrations ($n = 19$). Values that indicate a strong correlation (i.e., $r \geq 0.8$) are in bold.

	Na ⁺	NH ₄ ⁺	K ⁺	Mg ²⁺	Ca ²⁺	Cl ⁻	SO ₄ ²⁻	NO ₃ ⁻	EC	WSOC	OC
NH ₄ ⁺	0.28										
K ⁺	0.38	0.87									
Mg ²⁺	0.84	0.51	0.63								
Ca ²⁺	0.80	0.04	0.23	0.79							
Cl ⁻	0.85	0.32	0.41	0.83	0.77						
SO ₄ ²⁻	0.57	0.88	0.86	0.77	0.47	0.58					
NO ₃ ⁻	0.41	0.81	0.77	0.67	0.35	0.42	0.83				
EC	-0.22	0.23	0.22	-0.26	-0.28	-0.22	0.10	0.03			
WSOC	-0.04	0.17	0.12	-0.10	0.10	-0.03	0.16	0.17	0.59		
OC	-0.01	0.16	0.14	-0.05	0.17	-0.01	0.18	0.23	0.56	0.99	
TON	-0.10	0.81	0.61	0.16	-0.16	-0.08	0.65	0.67	0.51	0.45	0.43

[Title Page](#)[Abstract](#)[Introduction](#)[Conclusions](#)[References](#)[Tables](#)[Figures](#)[Full Screen / Esc](#)[Printer-friendly Version](#)[Interactive Discussion](#)

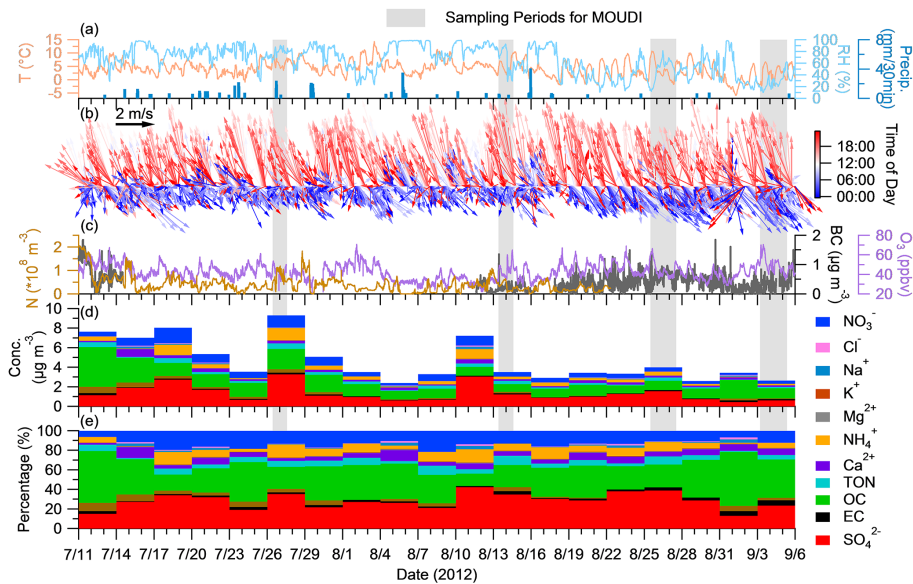


Figure 1. Time series for the **(a)** meteorological data, **(b)** wind speed and wind direction colored by time of day (BJT), **(c)** parallel instrument datasets including particle number concentration (N , $0.25 < d < 32 \mu\text{m}$), black carbon (BC), and O_3 , **(d)** mass concentration of water soluble ions, organic carbon (OC), elemental carbon (EC), and total organic nitrogen (TON), and **(e)** mass contribution of these species in **(d)**.

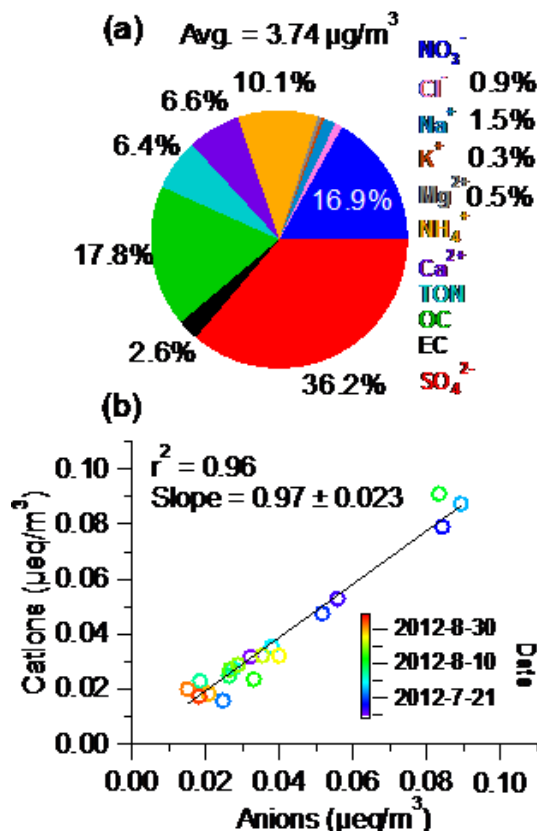


Figure 2. (a) The average composition of the species analyzed and (b) the charge balance between the cations ($\text{Na}^+ + \text{NH}_4^+ + \text{K}^+ + \text{Mg}^{2+} + \text{Ca}^{2+}$) and anions ($\text{Cl}^- + \text{SO}_4^{2-} + \text{NO}_3^-$).

[Title Page](#)[Abstract](#)[Introduction](#)[Conclusions](#)[References](#)[Tables](#)[Figures](#)[◀](#)[▶](#)[◀](#)[▶](#)[Back](#)[Close](#)[Full Screen / Esc](#)[Printer-friendly Version](#)[Interactive Discussion](#)

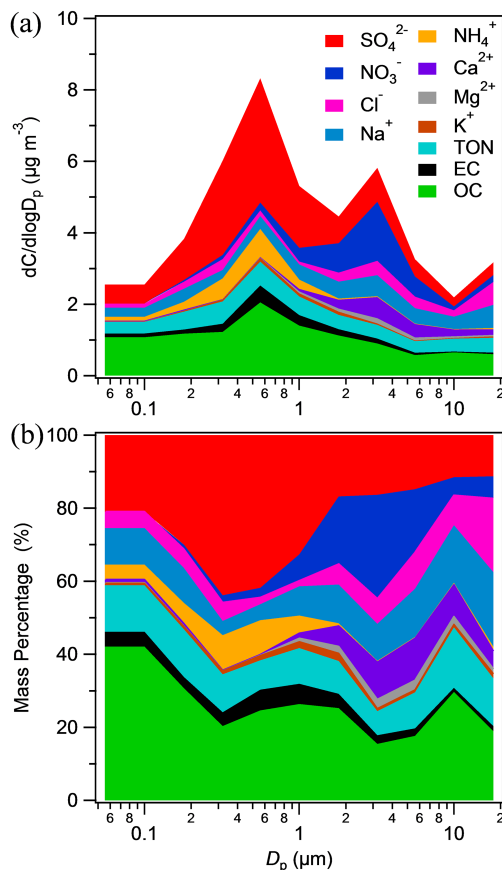


Figure 3. Average size distribution for (a) mass concentration and (b) mass percentage of water soluble inorganic ions (SO_4^{2-} , NO_3^- , Cl^- , NH_4^+ , Ca^{2+} , Mg^{2+} , and K^+), Total Organic Nitrogen (TON), elemental carbon (EC) and organic carbon (OC).

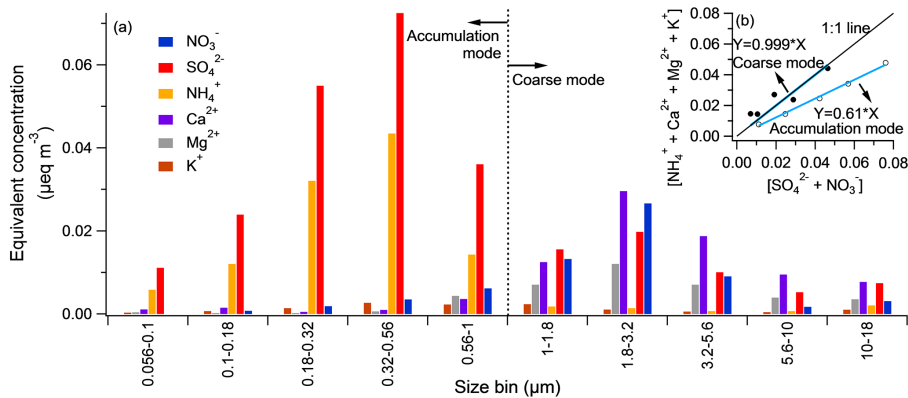


Figure 4. (a) Average equivalent concentration distributions of the water soluble inorganic species in individual size bins. The vertical dashed line indicates the boundary between the accumulation mode and the coarse mode. (b) Scatter plot of $[\text{NH}_4^+ + \text{Ca}^{2+} + \text{Mg}^{2+} + \text{K}^+]$ and $[\text{SO}_4^{2-} + \text{NO}_3^-]$ in the accumulation mode and coarse mode particles.

- [Title Page](#)
- [Abstract](#) [Introduction](#)
- [Conclusions](#) [References](#)
- [Tables](#) [Figures](#)
- [◀](#) [▶](#)
- [◀](#) [▶](#)
- [Back](#) [Close](#)
- [Full Screen / Esc](#)
- [Printer-friendly Version](#)
- [Interactive Discussion](#)

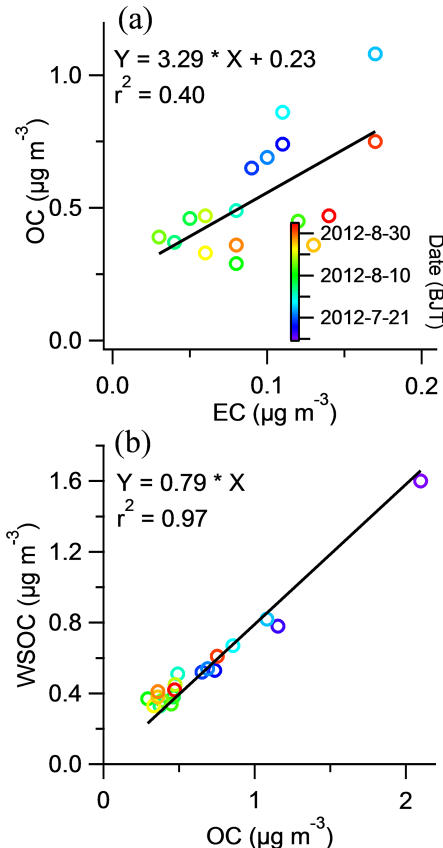


Figure 5. Scatter plots of (a) the organic carbon (OC) concentration against the elemental carbon (EC) concentration and (b) the water soluble organic carbon concentration (WSOC) against the OC colored by the sampling date.

[Title Page](#)[Abstract](#)[Introduction](#)[Conclusions](#)[References](#)[Tables](#)[Figures](#)[◀](#)[▶](#)[◀](#)[▶](#)[Back](#)[Close](#)[Full Screen / Esc](#)[Printer-friendly Version](#)[Interactive Discussion](#)

Insights into the chemical composition of summertime PM_{2.5}

J. Xu et al.

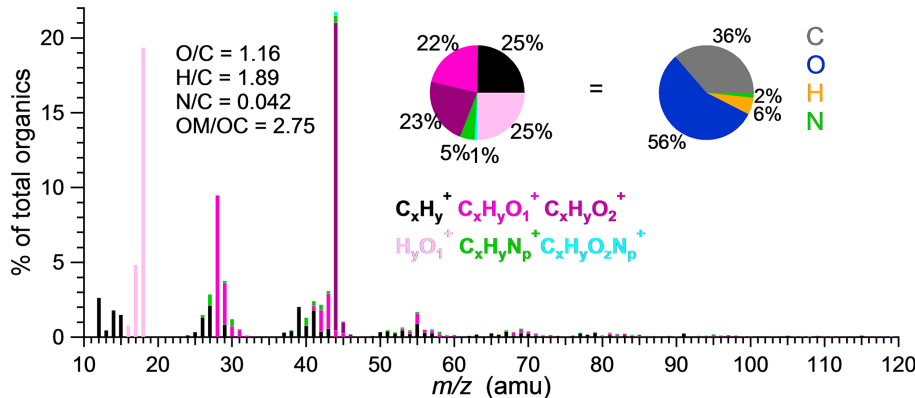


Figure 6. Average water soluble organic carbon (WSOM) mass spectrum and mass concentration fraction (pie charts) colored by the contributions of six ion categories and elements (C, O, H, and N).

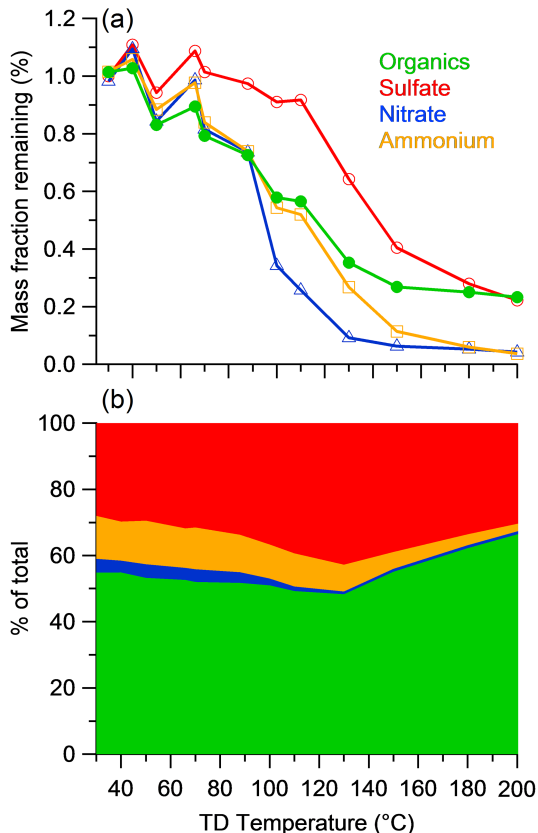


Figure 7. Thermal denuder profile for the organic species, sulfate, nitrate, and ammonium **(a)** by the remaining mass fraction **(b)** by the mass contribution.

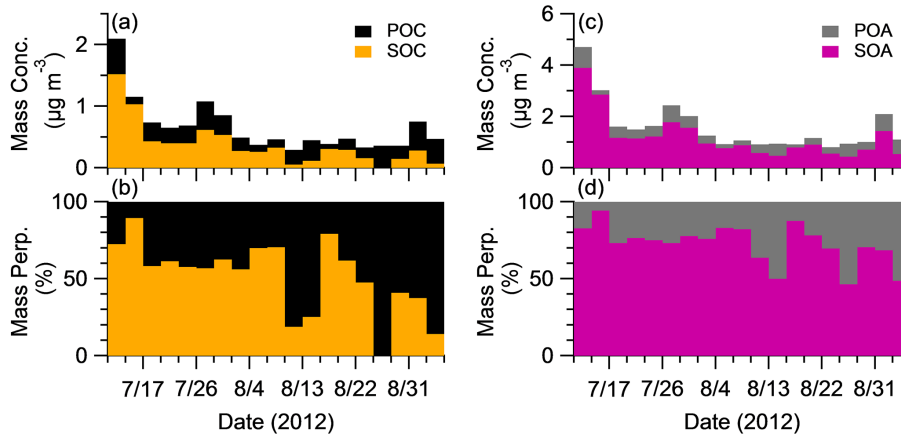


Figure 8. Estimations of (a and b) the primary and secondary organic carbon concentrations (Conc.) and contributions (Prop.) and (c and d) primary and secondary organic aerosol concentrations and contributions to the aerosol.